PNAS
www.pnas.org

Supplementary Information for

The 17-year spatiotemporal trend of $PM_{2.5}$ and its mortality burden in China

Fengchao Liang [a,b], Qingyang Xiao [c], Keyong Huang [b], Xueli Yang [b], Fangchao Liu [b], Jianxin Li [b], Xiangfeng Lu [b], Yang Liu [d,*], Dongfeng Gu [a,b,e,*]

[a] Key Laboratory of Cardiovascular Epidemiology, Chinese Academy of Medical Sciences, Beijing 100037, China; [b] Department of Epidemiology, Fuwai Hospital, National Center for Cardiovascular Diseases, Chinese Academy of Medical Sciences and Peking Union Medical College, Beijing 100037, China; [c] School of environment, Tsinghua University, Beijing 100084, China; [d] Gangarosa Department of Environmental Health, Rollins School of Public Health, Emory University, Atlanta, Georgia 30322, USA; [e] Medical school, Southern University of Science and Technology, Shenzhen 518055, China.

* Correspondence to:
Yang Liu and Dongfeng Gu
Email: yang.liu@emory.edu (Y.L.); gudongfeng@cashq.ac.cn (D.G.)

This PDF file includes:

Figs. S1 to S10
Tables S1 to S2

www.pnas.org/cgi/doi/10.1073/pnas.1919641117

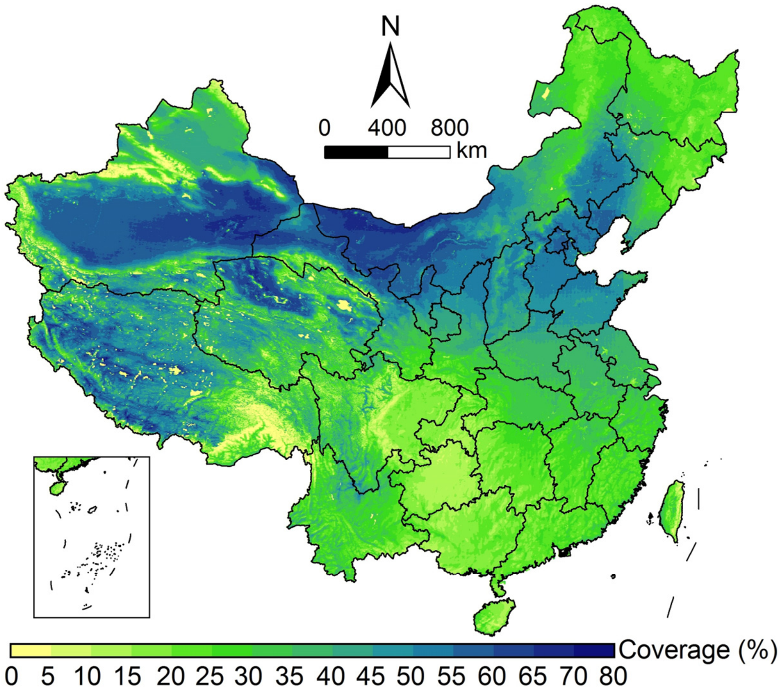

Fig. S1. Coverage of the Multi-Angle Implementation of Atmospheric Correction (MAIAC) aerosol optical depth (AOD) at the daily level from 2000 to 2016.

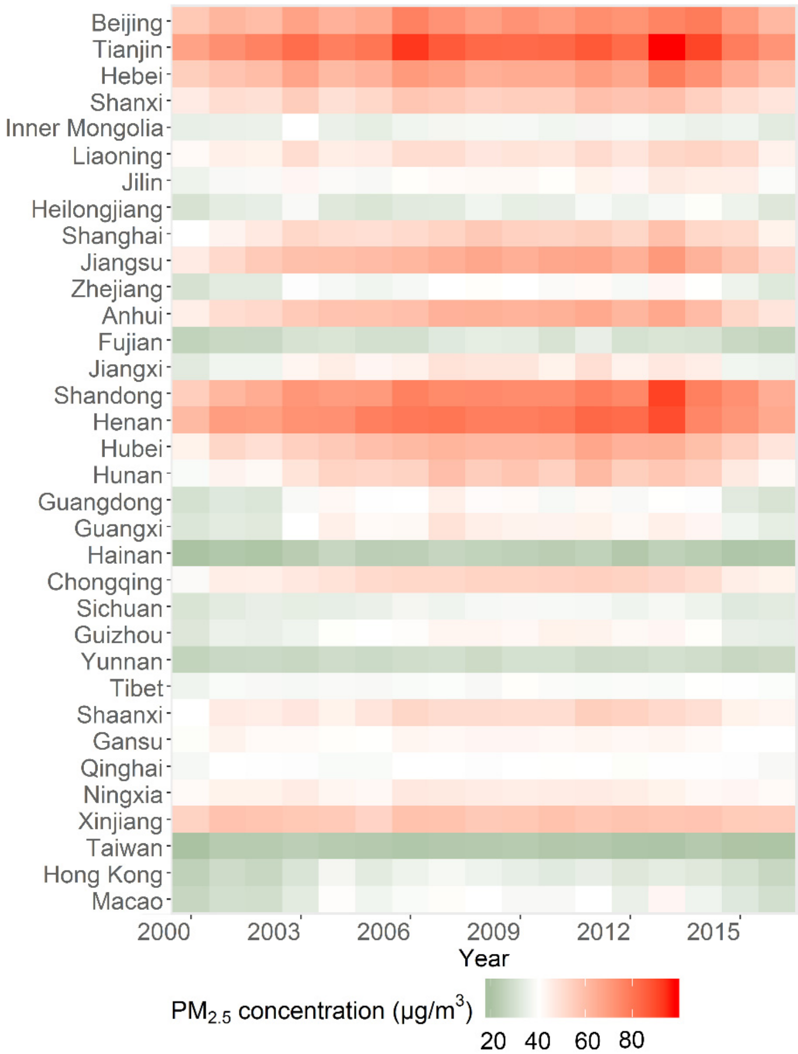

Fig. S2. Province-level spatiotemporal trends of annual mean $PM_{2.5}$ concentrations in China.

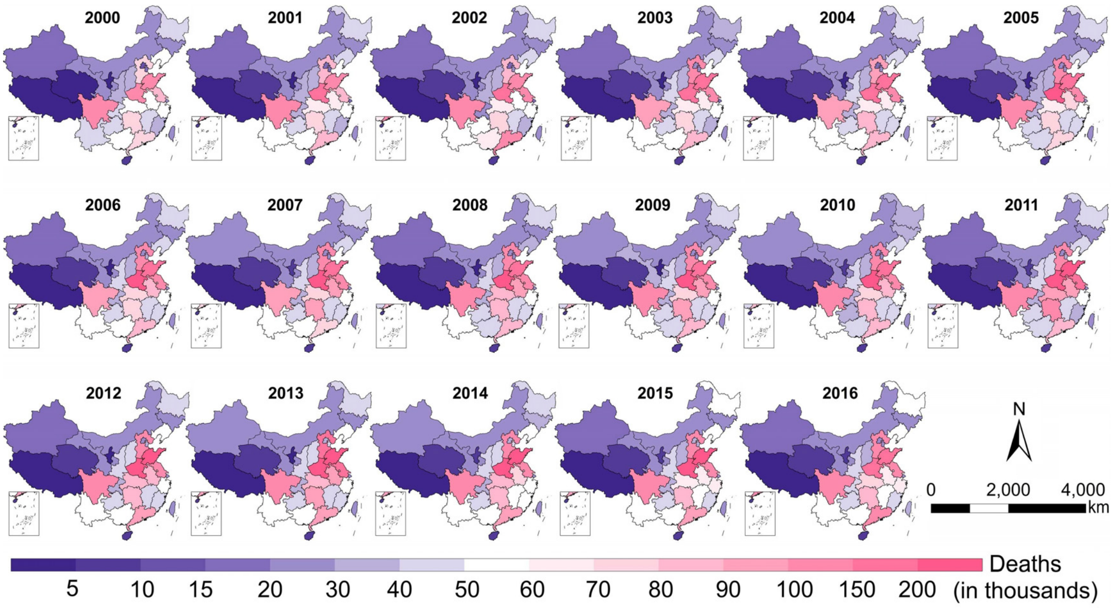

Fig. S3. Absolute number of annul premature deaths attributable to long-term $PM_{2.5}$ exposure in China from 2000 to 2016.

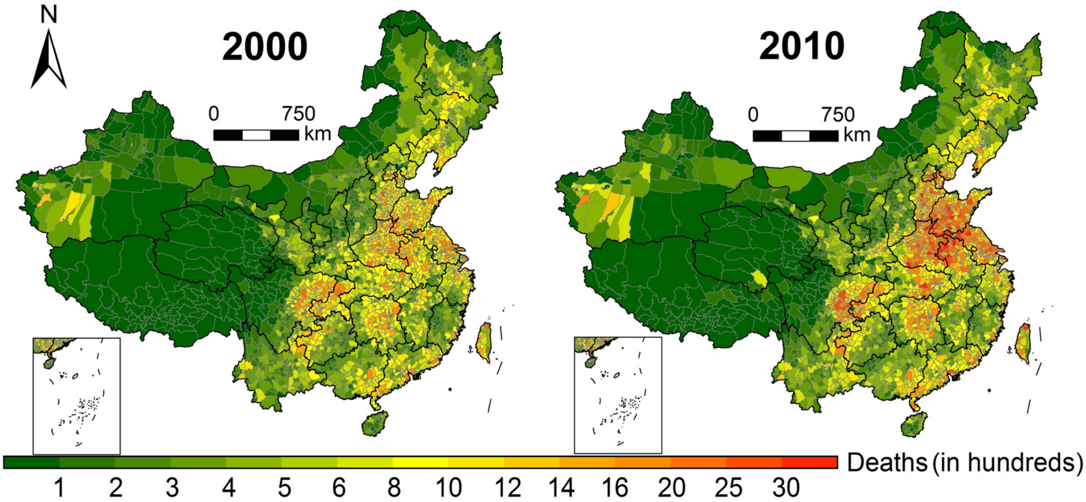

Fig. S4. County-level annual premature deaths attributable to long-term $PM_{2.5}$ exposure in China in 2000 and 2010.

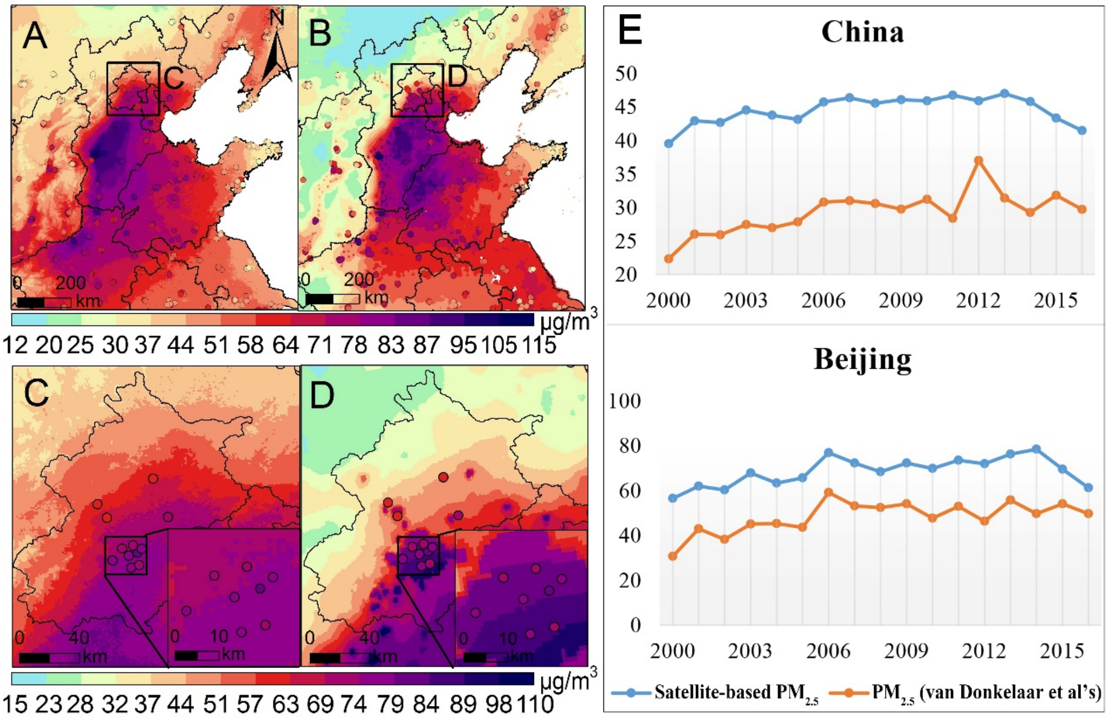

Fig. S5. Spatial and temporal comparisons of annual mean $PM_{2.5}$ concentrations estimated by the present work and van Donkelaar et al. A and B are the annual mean $PM_{2.5}$ concentrations in North China Plain in 2016 estimated by our study and van Donkelaar et al, respectively. C and D are the annual mean $PM_{2.5}$ concentrations in Beijing in 2016 estimated by our study and van et al, respectively. Circles in A, B, C, and D are annual mean $PM_{2.5}$ measurements from ground monitors in 2016. E shows the temporal trends of annual mean $PM_{2.5}$ concentrations in China and Beijing from 2000 to 2016.

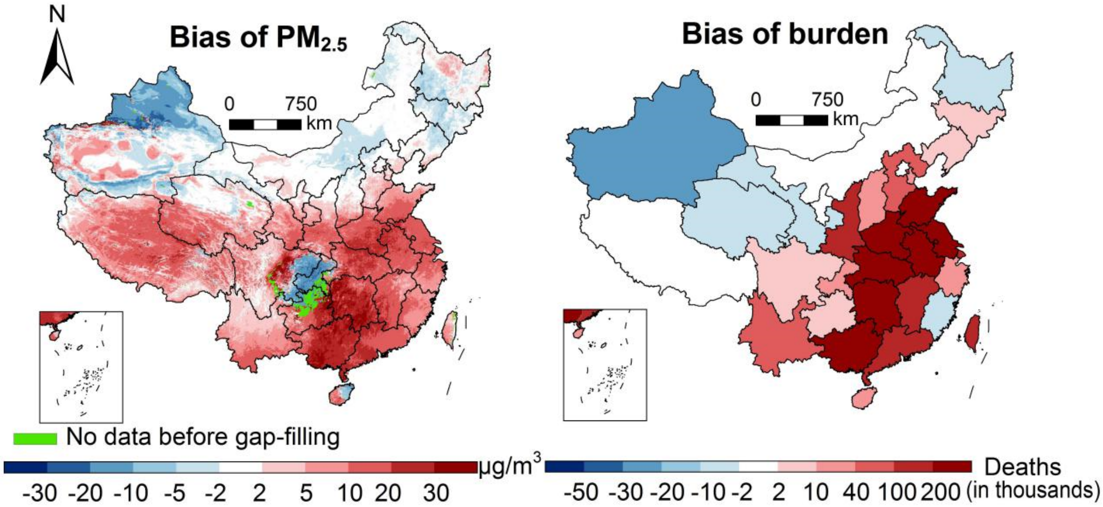

Fig. S6. Estimated biases of long-term $PM_{2.5}$ concentrations and premature deaths attributable to $PM_{2.5}$ exposures using satellite-based $PM_{2.5}$ estimates without filling missingness in AOD (during 2000 and 2016). Machine-learning models were re-run using all predictors in the main models, except that the original AOD data with missingness were used instead of the gap-filled AOD. Thereafter, mortality burden of adults in each province of China during 2000 and 2016 was calculated. The estimated bias of $PM_{2.5}$ estimation was presented as difference between 17-year averaged $PM_{2.5}$ estimates before gap-filling and those after gap-filling. The estimated bias of mortality burden was presented as the difference between estimated mortality burden using non-filled $PM_{2.5}$ concentrations and that using gap-filled $PM_{2.5}$.

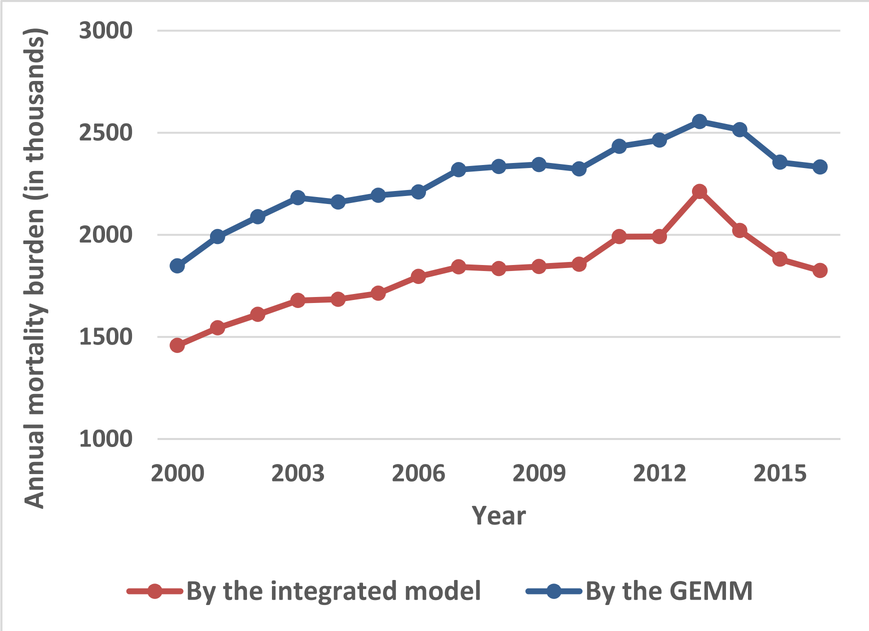

Fig. S7. Annual mortality burden estimated by our exposure-response curve and the Global Exposure Mortality Model (GEMM).

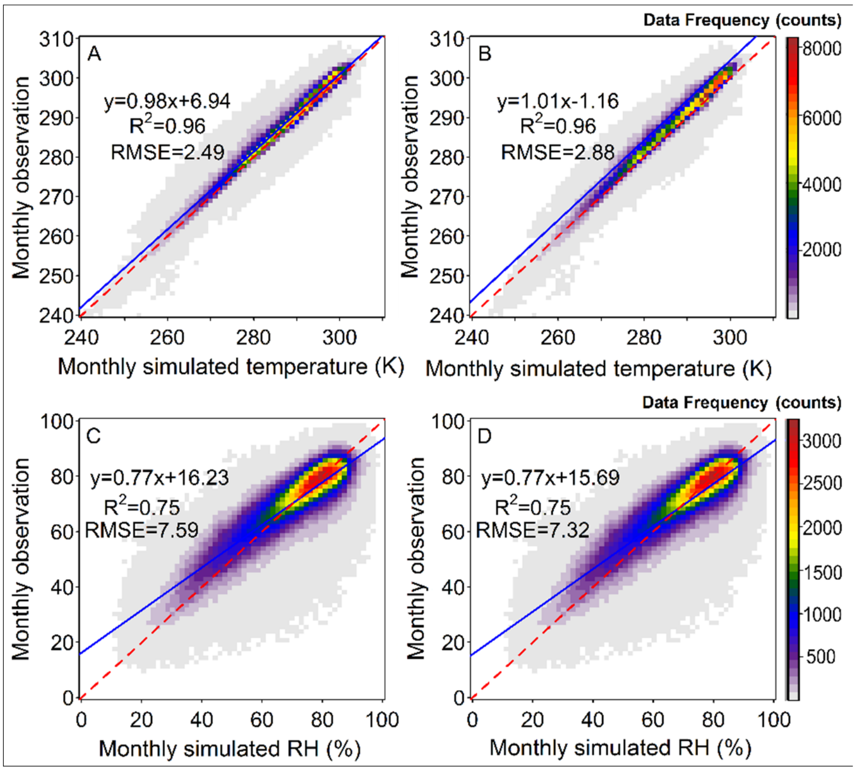

Fig. S8. Comparisons of cross-validation generated temperature and relative humidity (RH) and ground measurements using inverse distance weighting (IDW) and Ordinary Kriging. A and B are cross-validation performances for temperature by the IDW approach and the Ordinary Kriging model, respectively; C and D are cross-validation performances for relative humidity by the IDW approach and the Ordinary Kriging model, respectively.

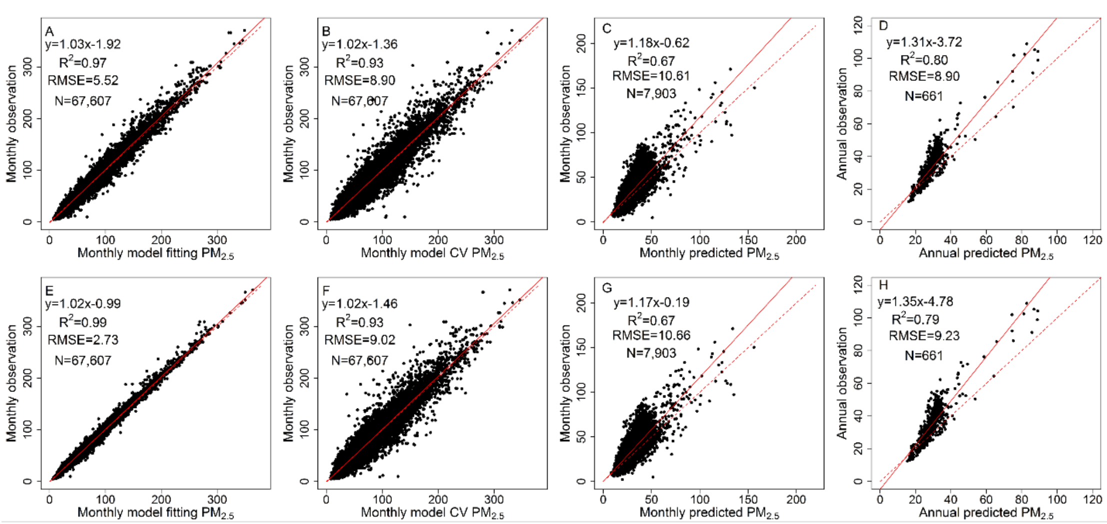

Fig. S9. Model fitting, cross-validation and predictive performances for arithmetic averaging and Bayesian model averaging. A to D are performances of arithmetic averaging and E to H are performances of Bayesian model averaging. A and B are model fitting, model cross-validation performances of the arithmetic averaging (2013-2016) at the monthly level, respectively; C and D are predictive performances at the monthly and annual levels for arithmetic averaging (2000-2012), respectively; E and F are model fitting and cross-validation performances of the Bayesian model averaging (2013-2016) at the monthly level, respectively; G and H are predictive performances at the monthly and annual levels for Bayesian model averaging (2000-2012), respectively.

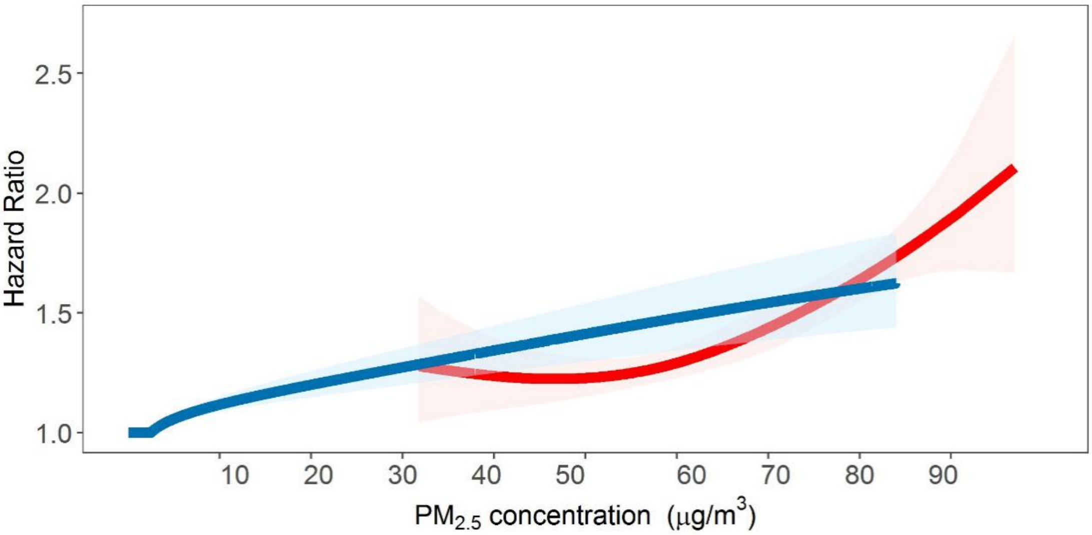

Fig. S10. The exposure-response curve for long-term $PM_{2.5}$ exposure and adult mortality. Blue curve and shading are function from the Global Exposure Mortality Model (GEMM) and its 95% confidence interval. Red curve and red shading are the concentration-response function and 95% confidence interval in China calibrated using the reference value (i.e., the health effect modeled by the GEMM at 31.2 μg/m^3). Effect modeled by the GEMM was calculated as:

$$\mathrm{HR(C)} = \exp\left\{\frac{\theta\log\left(\frac{z}{\alpha}+1\right)}{1+\exp\left(-\frac{z-\mu}{\nu}\right)}\right\}, where\ z = max(0, C - 2.4\ \mu g/m^3)$$

Where $\mathrm{HR(C)}$ is the hazard ratio of non-accident mortality under annual mean $PM_{2.5}$ concentration. In this model, 2.4 μg/m^3 was used as a counterfactual concentration, below which the hazard ratio of mortality associated with $PM_{2.5}$ exposure was assumed to be constant (i.e., Hazard Ratio=1.00); z is the max concentration difference between zero and $(C - 2.4)$; θ, α, μ, ν are the modeled age-specific parameters.

Table S1. Detailed information about $PM_{2.5}$ observations from 2000 to 2012 used for historical validation.

Source	Region	Time period	N of sites	N of monthly observations
Hong Kong environmental protection department	Hong Kong	2000-2012	12	777
Taiwan environmental protection agency	Taiwan	2000-2012	73	6973
Tsinghua University	Beijing	2007-2008	2	77
The U.S. Embassy	Beijing	2008-2012	1	53
The U.S. Embassy	Shanghai	2011-2012	1	12
The U.S. Embassy	Guangzhou	2012	1	11

Table S2. Model cross-validation performances of random forest model, extreme gradient boosting model, and their prediction averages.

Cluster	Random forest model		Extreme gradient boosting model		Mean of the two model predictions	
	R^2	RMSE	R^2	RMSE	R^2	RMSE
Overall	0.93	9.32	0.93	9.11	0.93	8.90
Southeast	0.93	6.54	0.93	6.29	0.93	6.18
Qinghai-Tibet	0.90	8.70	0.91	8.16	0.91	8.12
North	0.92	11.81	0.91	11.97	0.92	11.53
Northeast	0.90	9.72	0.91	9.08	0.91	9.06
Northwest	0.85	17.53	0.86	17.00	0.87	16.29
PRD	0.91	6.75	0.93	6.24	0.93	6.23
YRD	0.93	9.18	0.93	9.12	0.93	8.88

R^2, coefficient of determination; RMSE, root mean squared prediction error; PRD, Pearl River Delta; YRD, Yangtze River Delta.

.